Carbon cycle history through the Middle Jurassic (Aalenian– Bathonian) of the Mecsek Mountains, Southern Hungary

GREGORY D. PRICE[1], ISTVÁN FŐZY[2], and ANDRAS GALÁCZ[3]

[1]School of Geography, Earth & Environmental Sciences, University of Plymouth, Drake Circus, Plymouth, PL4 8AA, United Kingdom (g.price@plymouth.ac.uk)

[2]Department of Palaeontology and Geology, Hungarian Natural History Museum, POB 137, Budapest, H-1431 Hungary (fozy.istvan@nhmus.hu)

[3]Department of Palaeontology, Eötvös Loránd University, Pázmány P. sétány 1/C, Budapest, H-1117 Hungary (galacz@ludens.elte.hu)

Corresponding Author: Gregory D. Price, email g.price@plymouth.ac.uk; tel: +44 1752 584771; fax: +44 1752 584776

Abstract. A carbonate carbon isotope curve from the Aalenian–Bathonian interval is presented from the Óbánya valley, of the Mecsek Mountains, Hungary. This interval is certainly less well constrained and studied than other Jurassic time slices. The Óbánya valley lies in the eastern part of the Mecsek Mountains, between Óbánya and Kisújbánya and provides exposures of an Aalenian to Lower Cretaceous sequence. It is not strongly affected by tectonics, as compared to other sections of eastern Mecsek of the same age. In parts, a rich fossil assemblage has been collected, with Bathonian ammonites being especially valuable at this locality. The pelagic Middle Jurassic is represented by the Komló Calcareous Marl Formation and thin-bedded limestones of the Óbánya Limestone Formation. These are overlain by Upper Jurassic siliceous limestones and radiolarites of the Fonyászó Limestone Formation. Our new data indicate a series of carbon isotope anomalies within the late Aalenian and early-middle Bajocian. In particular, analysis of the Komló Calcareous Marl Formation reveals a negative carbon isotope excursion followed by positive values that occurs near the base of the section (across the Aalenian–Bajocian boundary). The origin of this carbon-isotope anomaly is interpreted to lie in significant changes to carbon fluxes potentially stemming from reduced run off, lowering the fertility of surface waters which in turn leads to lessened primary production and a negative $\delta^{13}C$ shift. These data are comparable with carbonate carbon isotope records from other Tethyan margin sediments. Our integrated biostratigraphy and carbon isotope stratigraphy enable us to improve stratigraphic correlation and age determination of the examined strata. Therefore, this study of the Komló Calcareous Marl Formation confirms that the existing carbon isotope curves serve as a global standard for Aalenian–Bathonian $\delta^{13}C$ variation.

Key words. Carbon, isotope stratigraphy, Aalenian, Bajocian, Óbánya, Mecsek, Hungary.

Introduction

The $\delta^{13}C$ curve of the Aalenian–Kimmeridgian interval shows a series of major Jurassic isotope events within the Aalenian, early-middle Bajocian, Callovian and middle Oxfordian (Hoffman et al. 1991; Bill et al. 1995; Weissert & Mohr 1996; Jenkyns 1996; Bartolini et al. 1999; Rey & Delgado 2002; O'Dogherty et al. 2006; Sandoval et al. 2008; Nunn et al. 2009; Price et al. 2016) recorded in both southern and northern Tethyan margin sediments. The potential of these $\delta^{13}C$ records for regional and global correlation of ancient marine sediments is evident. Some of these excursions (e.g. during the Oxfordian) are intrinsically coupled with climatic changes and have been extensively studied in many parts of the world (e.g. Bill et al. 1995; Jenkyns 1996). With respect to the Middle Jurassic interval (e.g. the Aalenian–Bathonian) it is the carbon isotope curves of Bartolini et al. (1999) and Sandoval et al. (2008) that often serve as a global standard (e.g. Ogg & Hinnov 2012). Major carbon-cycle perturbations in the Middle Jurassic are also recognised in terrestrial organic matter (fossil wood) (Hesselbo et al. 2003). Although the excursions of the Middle Jurassic have received only modest attention, they occur on more than one continent and may thus serve for global correlation of strata (e.g. Wetzel et al. 2013; Hönig & John 2015; Dzyuba et al. 2017). The goal of this study is to examine Aalenian – Bathonian carbon isotope stratigraphy from Hungary for comparison. A further aim of this study is to examine linkages between the $\delta^{13}C$ record of past global biotic and climatic change.

Geological Setting

The Lower Jurassic of the Mecsek Mountains of Hungary (Fig. 1) is characterized by coal bearing continental and shallow marine siliciclastic sediments (Haas et al. 1999). From Late Sinemurian times onwards, deposition consisted of deeper marine hemipelagic facies with mixed siliciclastic–carbonate lithologies (the Hosszúhetény and Komló Calcareous Marl formations, Raucsik & Merényi 2000). The site of this hemipelagic marly and calcareous marly sedimentation was most probably on or distally beyond the northern outer shelf of the Tethys Ocean (Fig. 2), whilst shallower conditions occurred towards the western margins (Enay et al. 1993). Although the precise age of the Komló Calcareous Marl Formation is uncertain, an Aalenian to Bajocian age is indicated (Forgó et al. 1966, Fig. 3). Overlying the Komló Calcareous Marl Formation, in the Mecsek, is the pelagic Bathonian–Callovian Óbánya Limestone Formation consisting of thin-bedded limestones and marls (Galácz 1994). The Upper Jurassic is represented by a siliceous limestone and radiolarite (the Fonyászó Limestone) as well as thin-bedded limestone (the Kisújbánya and Márévár limestones).

The Óbánya valley (Fig. 1) lies in the eastern part of the Mecsek Mountains, between Óbánya and Kisújbánya and provides exposures of the Komló Calcareous Marl Formation. The succession is not strongly affected by tectonics, as compared to other sections of eastern Mecsek of the same age (Velledits et al. 1986). The exposed Aalenian and Bajocian sediments (the Komló Calcareous Marl Formation) can be seen as alternating limestone beds (0.2–0.5m) and laminated beds consisting of dark grey, spotted, bituminous, micaceous marls (Fig. 4). The laminated beds become harder upwards with increasing carbonate content (from 36 to 55%, Velledits et al. 1986). Aside from some bivalve and plant imprints within the lower part of the succession, an ammonite (*Ludwigia* sp.) has been found indicating an Aalenian age (Velledits et al. 1986). The total thickness of the Aalenian has been estimated by Velledits et al. (1986) to be ~75 m although only the top ~25m was exposed. Fossils from the middle part of the succession include the ammonites *Dorsetensia* (at ~105m) and *Stephanoceras* (indicative of the Humphriesianum Zone), bivalve moulds together with carbonized plant fragments (Velledits et al. 1986).. Age diagnostic ammonites (e.g. *Leptosphinctes*, *Adabofoloceras* of the Niortense Zone) are recorded within the upper part of the Komló Calcareous Marl (Velledits et al. 1986). The total thickness of sediments of Bajocian age is ~170 m. The Komló Calcareous Marl is overlain by a red calcareous marl and nodular limestone (Fig 4) rich in age diagnostic ammonites (e.g. *Parkinsonia, Morphoceras* and *Procerites*) and pelagic microfossils (Galácz 1994). This 20m thick formation (the Óbánya Limestone Formation) is of Bathonian age (Galácz 1994) and was deposited in a pelagic environment. During this time major flooding events also occur elsewhere in northern Europe, with a peak transgression at the Bajocian-Bathonian boundary (Hallam 2001).

Materials and methods

For this study, 273 bulk carbonate samples were derived from the outcrop of the Óbánya valley. Samples were taken from both marl and limestone lithologies (Fig. 5). The average spacing of samples was ~0.3m. Subsamples (250 to 400 micrograms) avoiding macrofossils and sparry calcite veins, were then analysed for stable isotopes using a GV Instruments Isoprime Mass Spectrometer with a Gilson Multiflow carbonate auto-sampler at Plymouth University. Isotopic results were calibrated against the NBS-19 international standard. Reproducibility for both $\delta^{18}O$ and $\delta^{13}C$ was better than ±0.1‰, based upon duplicate sample analyses.

Results

The isotope results are presented in Figures 6 and 7. As isotopic analyses were undertaken from both marl and limestone lithologies a comparison of the isotopic composition of the two lithologies can be made. For the limestone (n = 181) the mean $\delta^{13}C$ value is 1.0‰ and -3.5‰ for $\delta^{18}O$. For the marl (n = 92) the mean $\delta^{13}C$ value is less positive, 0.4‰ and -4.3‰ for $\delta^{18}O$. The greater number of limestone vs. marl samples analysed reflects the generally better exposure of the limestones and poorer quality of the marl outcrops. It is for this reason that the carbon isotope curve (Fig. 7) is plotted though the limestone data only. Using Student's T-Test the isotopic difference between limestones and marls is also significant (at $p < .05$). These data are also consistent with stable isotope data from Raucsik (1997) who also isotopically analysed both limestone and marlstone carbonate samples from the Komló Calcareous Marl Formation (Fig. 6).

With respect to the carbon isotope stratigraphy (derived from the limestone data) a number of features of the curve are of particular note. Firstly, there is a negative excursion followed by positive values occurring near the base of the section (across the Aalenian–Bajocian boundary). The carbon-isotope values then become more positive, reaching the most positive values seen (at about 100 m height in Fig. 7). Although showing a good deal of scatter, values remain fairly positive, until towards the top of the Komló Calcareous Marl Formation where there is a drop in^{13}C values (at 166m). Carbon isotope values then increase again, where they reach a maximum (of 2.4 ‰), within the Bathonian. The carbon isotope data derived from the marls also follow this trend.

The wide range of oxygen isotopes and the low values, possibly points to a diagenetic overprint. Although a temperature control on oxygen isotopes cannot be excluded (see below), deep burial diagenesis and precipitation of calcite cement, commonly results in depleted in $\delta^{18}O$ values (Hudson 1977; Weissert, 1989: Hönig & John 2015). The preservation of $\delta^{13}C$ values or trends during carbonate diagenesis is, however, quite typical, and is likely due to the buffering effect of carbonate carbon on the diagenetic system, as this is the largest carbon reservoir (e.g., Scholle & Arthur 1980; Weissert, 1989). Hence, with respect to the oxygen isotope data, a diagenetic overprint affecting the samples analysed and results is likely. Although showing some scatter, oxygen isotope values remain fairly negative at the base of the section (the Aalenian) and become increasingly more positive upsection. The most positive oxygen isotope values are identified in the Bathonian (the Óbánya Limestone Formation).

Discussion

Limestone–marl alternations

The conspicuous limestone–marl alternations of the Komló Calcareous Marl Formation are likely to be caused by temporal variations in environmental parameters. It is generally accepted that the cause of the cyclical alternation of limestone beds and marls represents a direct response to changes in environmental conditions, such as productivity cycles (e.g. Wendler et al. 2002); dilution, i.e. changes in the influx of terrigenous non-carbonate material (e.g. Raucsik 1997; Weedon & Jenkyns 1999) or changes in input of carbonate mud from adjacent shallow-water carbonate factories (e.g. Pittet & Strasser 1998). Based on stable isotope data, Raucsik (1997) suggested that the higher $\delta^{13}C$ of the limestones was associated with higher productivity, whilst terrigenous dilution may have formed the limestone-marlstone alternation. Given that the data presented here are consistent with the data of Raucsik (1997), in that the limestones typically record more positive $\delta^{13}C$ values (Fig. 6), the same conclusion could be reached. A similar pattern could also be related to relatively short term changes in the export of neritic carbonate mud, as the $\delta^{13}C$ of neritic muds, derived from relatively shallow waters, tend to show more positive values than carbonate ooze produced by planktonic organisms (e.g. Swart & Eberli, 2005). Indeed, Bajocian shallow-water carbonate factories on the southern Tethyan shelf (Leinfelder et al. 2002) are likely to show relatively positive carbon isotope values, although are somewhat distal to the study site of hemipelagic sedimentation on northern outer shelf of the Tethys Ocean (Fig. 2). The Bajocian was a time of widespread oolite formation along the Northern (and southern) Tethys margin (Wetzel et al. 2013). Isotope values from these Northern Tethyan oolites (Wetzel et al. 2013) do not show particularly positive values expected for aragonite oolites. Indeed textures indicate that these oolites were calcitic (Wetzel et al. 2013) (i.e. a calcite sea sensu Sandberg, 1983) and therefore this region exporting aragonite during this time appears unlikely. Of note is that the oxygen isotope data for the marls are more negative than the data derived from the limestones (Fig. 6), a pattern consistent with carbonate ooze produced in relatively warm surface waters.

Bodin et al. (2016), have also suggested lithological, rather than oceanographic controls on $\delta^{13}C$ trends (e.g. during the earliest Toarcian of Morocco), whereby neritic $\delta^{13}C_{micrite}$ signatures show more positive values than carbonate ooze produced by planktonic organisms. Changes in carbon isotope values in marine carbonate successions have also been attributed to changes in organic matter remineralization and subaerial exposure around hardgrounds and subsequent carbonate precipitation from meteorically influenced fluids (e.g. Immenhauser et al. 2002; Hönig &

John 2015). Evidence for subaerial exposure (e.g. signs of palaeokarst) was not observed in the Óbánya valley.

Climatic and eustatic influences on carbon cycle changes

The negative excursion followed by positive values that occurs near the base of the section (across the Aalenian–Bajocian boundary), observed in this study, appears to correlate with a major carbon cycle perturbation recognized elsewhere (Fig. 8) as a widespread phenomenon on the basis of its carbon–isotope expression in both oceanic (Bartolini et al. 1996; O'Dogherty et al. 2006; Sucheras-Marx et al. 2012; Hönig & John 2015) and terrestrial reservoirs (Hesselbo et al. 2003). It cannot be excluded that an earlier negative excursion followed by positive values occurring in the Aalenian Concavum Zone at Agua Larga (O'Dogherty et al. 2006; Sandoval et al. 2008), is correlatable with the lowermost negative excursion. However, this possibility is not favoured as no sizable negative shift is located above, in the Bajocian part of the sucession. Carbon isotopes reach their most positive values, within the Óbánya succession, during the Early to mid-Bajocian, before declining across the Bajocian-Bathonian boundary. This same trend, is seen, for example in the Terminilletto section, Apennines, Italy (Bartolini et al. 1999) and the Betic Cordillera of southern Spain (O'Dogherty et al. 2006). Although there are evident differences in facies between these sections, due to deposition under differing conditions across the Tethys Ocean, the $\delta^{13}C$ signatures are similar. The carbon-isotope trends are therefore likely to represent at least supraregional perturbations in the carbon cycle. Hence, wide scale mechanisms need to be considered to account for the observed trends.

Gradual negative carbon isotope excursions in the geological record have, for example, been explained by reduced primary production (e.g. Weissert & Channell 1989) whereby, increasingly oligotrophic conditions, caused by reduced run off and nutrient fluxes to the oceans, lower the fertility of surface waters which in turn leads to lessened primary production and a negative $\delta^{13}C$ shift. Such a mechanism for $\delta^{13}C$ decreases has been associated with regressive conditions in the latest Jurassic Tethyan seaway (e.g. Weissert & Channell 1989; Tremolada et al., 2006). During the Aalenian-Bajocian boundary interval $\delta^{13}C$ decreases have also been correlated with regressive intervals (Sandoval et al. 2008). O'Dogherty et al. (2006) also point out the coincidence between carbon cycle perturbations and major changes in marine biota. For example the latest Toarcian–Early Aalenian is marked by the coexistence of very low radiolarian content, high proportions of the nannofossil *Schizosphaerella* spp., and moderate proportions of *C. crassus*, indicative of oligotrophic to mesotrophic palaeoceanographic conditions (Aguado et al. 2008). Although, there is no evidence of a regressive Aalenian-Bajocian boundary interval at Óbánya, a significant regressive event in Europe took place in Late Aalenian times (e.g. Hardenbol et al. 1998; Haq & Al-Qahtani, 2005) followed by Early Bajocian transgression and deepening (Hallam, 2001). As noted by Hallam (2001), Underhill & Partington (1993) demonstrated that the Aalenian eustatic sea-level fall in the Jurassic was in fact a phenomenon of regional tectonics. Within Europe the effects of an Early Bajocian transgression can be recognised widely, for example, in Morocco (Bodin et al. 2017), north eastern Spain (e.g. Aurell et al., 2003) and in the Jura Mountains of southern France (e.g. Razin et al. 1996).

Major perturbations in the carbon cycle have also been associated with pulses of magmatism (e.g. Wignall 2001; Hesselbo et al. 2003; Pálfy et al. 2001). However, the carbon isotope excursion reported here and any association with a large pulse of magmatism is not clearly demonstrated. For example, radiometric data from the Karoo basalts indicates that the main volume of the Karoo Large Igneous Province (LIP) was emplaced between 181 and 184 Ma (i.e. during the Late Pliensbachian to Early Toarcian) with limited late stage basaltic activity at 176 Ma (e.g. Jourdan et al. 2008). Younger episodic magmatic activity, associated with the break-up of Gondwana following the formation of the Karoo LIP, is reported from Patagonia and the Antarctic Peninsula (Pankhurst et al. 2000). Aalenian–Bathonian volcanism is also reported from the Crimea (Meijers et al. 2010), the Caucasus region (Odin et al. 1993) and Mexico (Rubio-Cisneros & Lawton 2011). Interestingly, the Aalenian–Early Bajocian interval also overlaps with the birth of the Pacific Plate and a major pulse of subduction related magmatism (Bartolini & Larson 2001; Koppers et al. 2003). Evidence for the impact of this magmatic activity can be assessed through $^{87}Sr/^{86}Sr$ data. The Aalenian–Early Bajocian seawater $^{87}Sr/^{86}Sr$ curve shows, however, a flat segment alluding to the limited impact of this magmatic activity. This contrasts with the relatively rapid fall in the seawater $^{87}Sr/^{86}Sr$ ratio seen through the Late Bathonian and Early Callovian (Wierzbowski et al. 2012). Hence it appears likely that the volcanogenic CO_2 associated with these events certainly represents a potential source for light carbon, although possibly not of sufficient magnitude and sufficiently light to achieve the observed isotopic change.

Alternatively, an injection of isotopically light carbon into the ocean and atmosphere from a remote source, such as methane from clathrates, wetlands, or thermal metamorphism organic rich sediments (e.g., McElwain et al. 2005; Bachan et al. 2012) has been considered as means to explain negative carbon isotope excursions. Similar events have been considered to have been a result of more regional events caused by recycling of isotopically light carbon from the lower water column (e.g. McArthur et al. 2008). However, that the Aalenian-Bajocian boundary event is observed in both marine (Fig. 8) and terrestrial settings (e.g. Hesselbo et al. 2003) has been considered to be an indication that the observed isotopic signals may have recorded a global (rather than regional) perturbation of the carbon cycle. As noted above, changes in the export of neritic carbonate mud (e.g. Swart & Eberli 2005) could also conceivably result in a negative isotope excursion in the geological record (e.g. Bodin et al. 2016; Ait-Itto et al. 2017). Hence a shift in the $\delta^{13}C_{micrite}$ signature is possible without any relation to variations in the global carbon isotope trend (Bodin et al. 2016; 2017). For this latter mechanism to be considered, sustained changes in the export of neritic mud are required to reach the study site and affect carbonate factories across Tethys. Furthermore, the negative excursion occurring in both oceanic and terrestrial reservoirs, provides an additional challenge for this to be a viable mechanism.

In contrast to the Aalenian-Bajocian boundary interval, more positive $\delta^{13}C$ values (Fig. 8) in the Early Bajocian Tethyan seaway could have been linked to warmer climates and rising sea levels, increased runoff and nutrient fluxes to the oceans, increasing the fertility of surface waters (e.g. Sandoval et al. 2008; Suchéras-Marx et al. 2012). For example Suchéras-Marx et al. (2012) show that calcareous nannofossil fluxes increase markedly (mainly related to the rise of *Watznaueria* genus) from the upper part of the Aalenian to the Early Bajocian, coinciding with a positive shift in carbon isotope compositions of bulk carbonate. High levels of CO_2 in the atmosphere could have also accelerated the transfer of nutrients from the continents to the oceans, through increasing weathering. Indeed, as noted above, significant injections of CO_2 have been associated with major pulses of subduction-related magmatism, linked to the opening of the Pacific Ocean and the breakup of Pangaea (e.g. Bartolini & Larson 2001). Equally, the evolution of Tethyan seawater temperatures during the Middle Jurassic period inferred from the oxygen isotopic composition of belemnite rostra, bivalve shells and from fish teeth (see Brigaud et al. 2009; Price, 2010) reveal warmth during the Early Bajocian and cooling from late Bajocian times through into the Bathonian. Also, the oxygen isotope data of this study (Fig. 7) broadly replicate this trend, whereby more negative values are seen in the lower part of the succession and more positive values are observed in the upper part of the section and within the Bathonian. Such a pattern of warming and cooling is consistent with an Early Bajocian transgression noted above.

Increasing $\delta^{13}C$ values in the Bajocian Tethyan seaway have also been linked to elevated productivity, as shown by radiolarian assemblages (Bartolini et al. 1999). O'Dogherty et al. (2006)

further point out ammonite radiations during the Early Bajocian, concomitant with increasing $\delta^{13}C$ values. The Early Bajocian positive excursion has also been correlated in the southern margin of western Tethys with a “carbonate production crisis” and concomitant with the onset of biosiliceous sedimentation in several basins (Bartolini et al. 1996). The Komló Calcareous Marl Formation shows, however, increasing carbonate content upwards (Velledits et al. 1986) rather than any marked decreases in carbonate. It is the Late Jurassic that sees biosiliceous sedimentation in the Óbánya valley (Velledits et al. 1986).

Conclusions

Our study of the Komló Calcareous Marl Formation of the Mecsek Mountains of Hungary reveals a negative carbon isotope excursion followed by positive values that occurs near the base of the section (across the Aalenian–Bajocian boundary). The origin of this carbon-isotope anomaly is interpreted to lie in significant changes to carbon fluxes stemming from changes in primary production linked to increasingly oligotrophic conditions, caused for example, by reduced run off and nutrient fluxes to the oceans, lowering the fertility of surface waters which in turn leads to lessened primary production and a negative $\delta^{13}C$ shift (e.g. O'Dogherty et al. 2006; Sandoval et al. 2008). That the Aalenian-Bajocian boundary carbon isotope event is observed in both marine and terrestrial settings (e.g. Hesselbo et al. 2003) indicates that the observed isotopic signals record global (rather than regional) perturbation of the carbon cycle. Changes in the export of neritic carbonate mud could also conceivably result in a negative isotope excursion, but this mechanism required sustained changes affecting carbonate factories across Tethys. Furthermore, the negative excursion occurring in both oceanic and terrestrial reservoirs, challenges this as a viable mechanism. In view of the gradual isotopic changes inferred from these Tethyan carbonates, an explanation in terms of the rapid dissociation of gas hydrates also appears unlikely. This study of the Komló Calcareous Marl Formation further confirms that the carbon isotope curves of Bartolini et al. (1999) and Sandoval et al. (2008), do indeed serve as a global standard for Aalenian–Bathonian $\delta^{13}C$ variation.

Acknowledgments This work has received support from the SYNTHESYS Project (http://www.synthesys.info/), financed by European Community Research Infrastructure Action under the FP6 Structuring the European Research Area Program. We thank Béla Raucsik for assistance with fieldwork. The manuscript was considerably improved by constructive reviews by Helmut Weissert and an anonymous reviewer.

References

Aguado R., O'Dogherty L. & Sandoval J., 2008: Fertility changes in surface waters during the Aalenian (mid-Jurassic) of the Western Tethys as revealed by calcareous nannofossils and carbon-cycle perturbations. *Marine Micropaleontology* 68, 268–285.

Ait-Itto F-Z., Price G.D., Addi, A.A., Chafiki D. & Mannani I., 2017: Bulk-carbonate and belemnite carbon-isotope records across the Pliensbachian-Toarcian boundary on the northern margin of Gondwana (Issouka, Middle Atlas, Morocco). *Palaeogeography Palaeoclimatology Palaeoecology* 466, 128–136.

Aurell M., Robles S., Badenas B., Rosales I., Quesada S., Melendez G. & Garcıa-Ramos J.C. 2003: Transgressive–regressive cycles and Jurassic palaeogeography of northeast Iberia. *Sedimentary Geology* 162, 239–271.

Bachan A., van de Schootbrugge B., Fiebig J., McRoberts C.A., Ciarapica C. & Payne J.L., 2012: Carbon cycle dynamics following the end-Triassic mass extinction: Constraints from paired δ^{13}Ccarb and δ^{13}Corg records. *Geochemistry, Geophysics, Geosystems* 13, Q09008. doi.org/10.1029/2012GC004150 1.

Bartolini A., Baumgartner P.O. & Hunziker J.C., 1996: Middle and Late Jurassic carbon stable-isotope stratigraphy and radiolarite sedimentation of the Umbria-Marche Basin (Central Italy). *Eclogae Geologicae Helvetiae* 89, 811–844.

Bartolini A., Baumgartner P.O. & Guex J., 1999: Middle and Late Jurassic radiolarian palaeoecology versus carbon-isotope stratigraphy. *Palaeogeography, Palaeoclimatology, Palaeoecology* 145, 43–60.

Bartolini A. & Larson R., 2001: The Pacific microplate and the Pangea supercontinent in the Early-Middle Jurassic. *Geology* 29, 735–738.

Bill M., Baumgartner P.O., Hunziker J.C. & Sharp, Z.D., 1995: Carbon isotope stratigraphy of the Liesberg Beds Member (Oxfordian, Swiss Jura) using echinoids and crinoids. *Eclogae Geologicae Helvetiae* 88 135–155.

Bodin S., Krencker F., Kothe T., Hoffmann R., Mattioli E., Heimhofer U. & Kabiri L., 2016: Perturbation of the carbon cycle during the late Pliensbachian – Early Toarcian: New insight from high–resolution carbon isotope records in Morocco. *Journal of African Earth Sciences* 116, 89–104.

Bodin S., Hönig, M.R., Krencker F-N., Danisch J. & Kabiri L. 2017: Neritic carbonate crisis during the Early Bajocian: Divergent responses to a global environmental perturbation. *Palaeogeography, Palaeoclimatology, Palaeoecology* 468, 184–199

Brigaud B., Durlet C., Deconinck J-F., Vincent B., Pucéat E., Thierry J. & Trouiller A., 2009: Facies and climate/environmental changes recorded on a carbonate ramp: A sedimentological and geochemical approach on Middle Jurassic carbonates (Paris Basin, France). *Sedimentary Geology*, 222,181–206

Dzyuba O.S., Guzhikov A.Yu., Manikin A.G., Shurygin B.N., Grishchenko V.A., Kosenko I.N., Surinskii, A.M., Seltzer V.B. & Urman O.S., 2017. Magneto- and carbon-isotope stratigraphy of the Lower–Middle Bathonian in the Sokur section (Saratov, Central Russia): implications for global correlation. *Russian Geology and Geophysics* 58, 206–224.

Enay R., Guiraud R., Ricou, L.E., Mangold C., Thierry J., Cariou E., Bellion Y. & Dercourt, J., 1993: Callovian palaeoenvironments (162 to 158 Ma). In: Dercourt, J., Ricou, L.E., Vrielynck, B. (Eds.), Atlas Tethys Palaeoenvironmental Maps. Maps. BEICIP-FRANLAB, Rueil-Malmaison

Forgó L. Moldvay L. Stefanovics P. & Wein, G., 1966: Explanatory notes to the 1:200000 scale geological map. Hungarian Geological Survey, Budapest, 1–196. [In Hungarian].

Főzy I. (Ed.) 2012: Lithostratigraphic units of Hungary. Jurassic. *Magyarhoni Földtani Társulat*, Budapest, pp. 235. [In Hungarian].

Galácz A., 1994: Ammonite stratigraphy of the Bathonian red, nodular marl in the Mecsek Mts (S Hungary). *Annales Universitatis Scientiarum Budapestinensis de Rolando Eötvös Nominatae, Sectio Geologica* 30, 115–150.

Haas J., Hámor G. & Korpás L., 1999: Geological setting and tectonic evolution of Hungary. *Geologica Hungarica series Geologica* 24, 179–196.

Hallam A., 2001: A review of the broad pattern of Jurassic sea-level changes and their possible causes in the light of current knowledge. *Palaeogeography Palaeoclimatology Palaeoecology* 167, 23–37.

Hardenbol J., Thierry J., Farley M.B., Jacquin T., De Graciansky P.C., Vail P.R., 1998: Mesozoic and Cenozoic sequence chronostratigraphic framework of European Basins. Jurassic sequence chronostratigraphy. In: De Graciansky, P.C., Hardenbol, J., Jacquin, J., Vail, P.R. (Eds.), Mesozoic and Cenozoic Sequence Stratigraphy of European Basins. SEPM Special Publication 60, chart 6.

Haq B.U. & Al-Qahtani A.M., 2005: Phanerozoic cycles of sea-level change on the Arabian Platform. *GeoArabia,* 10, 127–160.

Hesselbo S.P., Morgans-Bell H.S., McElwain J.C., Rees P.M., Robinson S.A. & Ross C.E., 2003. Carbon-Cycle Perturbation in the Middle Jurassic and accompanying changes in the terrestrial paleoenvironment. *Journal of Geology* 111, 259–276.

Hoffman A., Gruszczynski, M., Malkowski K., Halas S. Matyja B.A. & Wierzbowski, A., 1991: Carbon and oxygen isotope curves for the Oxfordian of central Poland. *Acta Geologica Polonica* 43 157–164.

Hönig M.R. & John, C.M., 2015: Sedimentological and isotopic heterogeneities within a Jurassic carbonate ramp (UAE) and implications for reservoirs in the Middle East. Marine and *Petroleum Geology* 68, 240–257.

Hudson J.D., 1977: Stable isotopes and limestone lithification. *Journal of the Geological Society of London* 133, 637–660.

Immenhauser A., Kenter J.A.M., Ganssen G., Bahamonde J.R., Van Vliet A. & Saher M.H., 2002: Origin and significance of isotope Shifts in Pennsylvanian Carbonates (Asturias, NW Spain). *Journal of Sedimentary Research*, 72, 82–94.

Jenkyns H.C., 1996: Relative sea-level change and carbon isotopes: data from the Upper Jurassic (Oxfordian) of central and Southern Europe. *Terra Nova* 8, 75–85.

Jourdan F., Féraud, G., Bertrand H., Watkeys M.K. & Renne P.R., 2008: ^{40}Ar/^{39}Ar ages of the sill complex of the Karoo large igneous province: implications for the Pliensbachian–Toarcian climate change. *Geochemical Geophysical Geosystem* 9, Q06009.

Koppers A.A.P., Staudigel H. & Duncan R.A., 2003: High-resolution ^{40}Ar/^{39}Ar dating of the oldest oceanic basement basalts in the western Pacific basin. *Geochemistry Geophysics Geosystems*, 4, Article Number: 8914, DOI: 10.1029/2003GC000574

Leinfelder R.R., Schmid, D.U., Nose M. & Werner W., 2002: Jurassic reef patterns: the expression of changing globe. In: Kiessling W, Flügel E, Golonka J (eds) Phanerozoic reef patterns. SEPM, Tulsa, Special Publication 72, 465–520.

McArthur J.M., Algeo T.J. van de Schootbrugge B., Li Q. & Howarth R.J., 2008: Basinal restriction, black shales, and the Early Toarcian (Jurassic) oceanic anoxic event. *Paleoceanography* 23, PA4217.

McElwain J.C., Wade-Murphy J. & Hesselbo S.P., 2005: Changes in carbon dioxide during an oceanic anoxic event linked to intrusion into Gondwana coals. *Nature* 435, 479–482.

Meijers M.J.M., Vrouwe B., Van Hinsbergen D.J.J., Kuiper K.F., Wijbrans J., Davies G.R., Stephenson R.A., Kaymakci N., Matenco L. & Saintot A., 2010: Jurassic arc volcanism on Crimea (Ukraine): Implications for the paleo-subduction zone configuration of the Black Sea region. *Lithos* 119, 412–426.

Némedi-varga Z., 1998: A Mecsek- és a Villányi Egység Jura képzõdményeinek rétegtana (The stratigraphy of the Jurassic units of the Mecsek Mountains and Villányi Mountains) in: Bérci I. Jámbor A. (eds), Magyarország geológiai képzõdményekinek rétegtana (The stratigraphy of the Hungarian geological units). MOL Hun. Oil Gas Comp. and Geol. Inst. Hun., Budapest 319–336 (in Hungarian).

Nunn E.V., Price G.D., Hart M. B., Page K.N. & Leng M.J. 2009: Terrestrial and marine carbon isotope signals from the Callovian–Kimmeridgian (Late Jurassic) succession at Staffin Bay, Isle of Skye, Scotland. *Journal of the Geological Society, London,* 166, 633–641.

Odin G.S., Gillot P.Y., Lordkipanidze M., Hernandez J. & Dercourt J., 1993: 1st datings of ammonite-bearing Bajocian suites from Caucasus (Georgia) – K-Ar ages of volcanic hornblendes. *Comptes Rendus de l Academie des Sciences Serie* ii 317, 629-638.

O'Dogherty L., Sandoval J., Bartolini A., Bruchez S., Bill M. & Guex J., 2006: Carbon–isotope stratigraphy and ammonite faunal turnover for the Middle Jurassic in the Southern Iberian palaeomargin. *Palaeogeography, Palaeoclimatology, Palaeoecology* 239, 311–333.

Ogg, J.G., Hinnov, L.A., 2012: Chapter 26 – Jurassic. In: Gradstein, F., Ogg, J., Schmitz, M., Ogg, G. (Eds.), The Geologic Time Scale 2012. Elsevier, Boston, pp. 731–791.

Pálfy J., Demény A., Haas J., Hetényi M., Orchard M.J. & Vető I., 2001: Carbon isotope anomaly and other geochemical changes at the Triassic–Jurassic boundary from a marine section in Hungary. *Geology* 29, 1047–1050.

Pankhurst R.J., Riley T.R., Fanning C.M. & Kelley S.P., 2000: Episodic silicic volcanism in Patagonia and the Antarctic Peninsula: Chronology of magmatism associated with the break-up of Gondwana. *Journal of Petrology* 41, 605–625.

Pittet B. & Strasser A., 1998: Depositional sequences in deep-shelf environments formed through carbonate-mud export from the shallow platform (Late Oxfordian, German Swabian Alb and eastern Swiss Jura). *Eclogae Geologicae Helvetiae* 91, 149–169.

Price G.D., 2010: Carbon–isotope stratigraphy and temperature change during the early–Middle Jurassic Toarcian – Aalenian), Raasay, Scotland, UK. *Palaeogeography Palaeoclimatology Palaeoecology* 285, 255–263.

Price G.D., Főzy, I. & Pálfy J., 2016: Carbon cycle history through the Jurassic–Cretaceous boundary: A new global $\delta^{13}C$ stack. *Palaeogeography, Palaeoclimatology, Palaeoecology* 451, 46-61.

Raucsik B., 1997: Stable isotopic composition of the Komló Calcareous Marl Formation ("spotted marl" s. str.), Mecsek Mountains, S. Hungary. Acta Mineralogica-Petrographica 38, 95-109.

Raucsik B. & Merényi L., 2000: Origin and environmental significance of clay minerals in the Lower Jurassic formations of the Mecsek Mts. Hungary. *Acta Geologica Hungarica* 43, 405–429.

Razin P., Bonijoly D., Le Strat P., Courel L., Poli E., Dromart G. & Elmi S., 1996: Stratigraphic record of the structural evolution of the western extensional margin of the Subalpine Basin during the Triassic and Jurassic, Ardeche, France. *Marine and Petroleum Geology* 13, 625–652.

Rey J. & Delgado A., 2002: Carbon and oxygen isotopes: a tool for Jurassic and early Cretaceous pelagic correlation (southern Spain). *Geological Journal* 37, 337–345.

Rubio-Cisneros I. & Lawton T.F., 2011: Detrital zircon U-Pb ages of sandstones in continental red beds at Valle de Huizachal, Tamaulipas, NE Mexico: Record of Early-Middle Jurassic arc volcanism and transition to crustal extension. *Geosphere* 7, 159-170.

Sandberg, P.A., 1983: An oscillating trend in Phanerozoic non-skeletal carbonate mineralogy. *Nature* 305, 19–22.

Sandoval J., O'Dogherty L., Aguado R., Bartolini A., Bruchez S. & Bill M., 2008: Aalenian carbon-isotope stratigraphy: Calibration with ammonite, radiolarian and nannofossil events in the Western Tethys. *Palaeogeography, Palaeoclimatology, Palaeoecology* 267, 115–137.

Scholle P.A. & Arthur M.A., 1980: Carbon isotope fluctuations in Cretaceous pelagic limestones: potential stratigraphic and petroleum exploration tool. *American Association of Petroleum Geologists Bulletin* 64, 67–87.

Suchéras-Marx B., Guihou A., Giraud F., Lécuyer C., Allemand P., Pittet B. & Mattioli E., 2012: Impact of the Middle Jurassic diversification of Watznaueria (coccolith-bearing algae) on the carbon cycle and $\delta^{13}C$ of bulk marine carbonates. *Global and Planetary Change* 86–87, 92–100.

Suchéras-Marx B., Giraud F., Fernandez V., Pittet B., Lecuyer C., Olivero D. & Mattioli E., 2013: Duration of the early Bajocian and the associated $\delta^{13}C$ positive excursion based on cyclostratigraphy. *Journal of the Geol. Soc.* 170, 107–118.

Swart P.K. & Eberli G.P., 2005: The nature of the $\delta^{13}C$ of periplatform sediments: Implications for stratigraphy and the global carbon cycle. *Sedimentary Geology* 175, 115–129.

Tremolada, F., Bornemann A., Bralower T.J., Koeberl C. & van de Schootbrugge B., 2006: Paleoceanographic changes across the Jurassic/Cretaceous boundary: The calcareous phytoplankton response. *Earth and Planetary Science Letters* 241, 361– 371.

Underhill J.R. & Partington M.A., 1993: Jurassic thermal doming and deflation: the sequence stratigraphic evidence. In: Parker, J.R. (Ed.): Petroleum Geology of North-West Europe: Proceedings of the 4th Conference, 337–345.

Velledits F., Híves T. & Bársony E., 1986: A Jurassic-Lower Cretaceous profile in Óbánya valley (Mecsek Mts. Hungary). *Annales Universitatis Scientiarum Budapestinensis de Rolando Eötvös Nominatae, Sectio Geologica* 26 159–175.

Weedon G.P. & Jenkyns H.C., 1999: Cyclostratigraphy and the Early Jurassic timescale: data from the Belemnite Marls, Dorset, south England. Geological Society of America Bulletin 111, 1823–1843.

Weissert, H. 1989: C-isotope stratigraphy as monitor of paleoenvironmental changes: A case study from the early Cretaceous. *Surveys in Geophysics* 10, 1–61.

Weissert H. & Channell, J.E.T., 1989: Tethyan carbonate carbon isotope stratigraphy across the Jurassic-Cretaceous boundary: an indicator of decelerated carbon cycling. *Paleoceanography* 4 483–494.

Weissert H. & Mohr H., 1996: Late Jurassic climate and impact on carbon cycling. *Palaeogeography, Palaeoclimatology, Palaeoecology* 122 27– 42.

Wendler J., Gräfe K-U. & Willems H., 2002: Reconstruction of mid-Cenomanian orbitally forced palaeoenvironmental changes based on calcareous dinoflagellate cycts. *Palaeogeography Palaeoclimatology Palaeoecology* 179 19–41.

Wetzel, A., Weissert, H., Schaub, M. & Voegelin, A.R., 2013: Sea-water circulation on an oolite-dominated carbonate system in an epeiric sea (Middle Jurassic, Switzerland). *Sedimentology*, 60, 19–35.

Wierzbowski H., Anczkiewicz R., Bazarnik J. & Pawlak J., 2012: Strontium isotope variations in Middle Jurassic (Late Bajocian–Callovian) seawater: Implications for Earth's tectonic activity and marine environments. *Chemical Geology* 334, 171–181.

Wignall P.B., 2001: Large igneous provinces and mass extinctions. *Earth-Science Reviews* 53, 1–33.

Figure Captions

Figure 1 A. Location map showing the location of the Óbánya valley within Hungary. Grey inset box shows location of the Mecsek Mountains. B. Distribution of Mesozoic volcanic and sedimentary units within the Mecsek Mountains from Galácz (1994).

Figure 2. Middle Jurassic palaeogeographic map of the Western Tethyan realm (modified from Enay et al. 1993), localities; 1– Óbánya, 2 Wadi Naqab, United Arab Emirates 3 – Southern Iberia, 4 – Umbria-Marche Basin (Central Italy), 5 – Cabo Mondego, Portugal, 6 – Chaudon Norante, SE France.

Figure 3. Lithostratigraphical scheme for the Jurassic deposits of the Mecsek Zone (Hungary) modified from Némedi Varga (1998) and Főzy (2012).

Figure 4 A, B, Sections of the Komló Calcareous Marl Formation in the Óbánya valley, (notebook for scale). C. The Óbánya Limestone Formation D. Upper Jurassic siliceous limestones and radiolarites the Fonyászó Limestone Formation.

Figure 5 A. Photomicrograph of the limestone lithology (from the Komló Calcareous Marl Formation) dominated by calcite microspar (sample OB115, scale bar 1 mm). Small patches of coarser sparry calcite may have formed as a cement during diagenesis within primary porosity or by neomorphism of aragonite. B. Photomicrograph of marl lithology (from the Komló Calcareous Marl Formation) showing abundant small sparry bioclasts, including crinoids within a micritic and organic rich matrix (sample OB546, scale bar 0.2 mm). C. Photomicrograph of the Óbánya Limestone Formation showing abundant sparry small bioclast fragments within a muddy matrix (sample OB125, scale bar 0.2 mm).

Figure 6. Cross plot of $\delta^{18}O$ and $\delta^{13}C$ data from the Aalenian– Bajocian interval, Óbánya valley, of the Mecsek Mountains, Hungary. Data from Raucsik (1997) is also shown.

Figure 7. Isotopic results ($\delta^{13}C$ and $\delta^{18}O_{micrite}$) from the Óbánya section. The ammonite data is from Velledits et al. (1986) and Galácz (1994). Zonal boundaries are not possible to identify because of very scattered occurrences of diagnostic ammonites. Crosses are the data derived from marls. The isotope curves (and 5 point running means) are plotted though the limestone data only.

Figure 8. Carbon isotope stratigraphies of the Aalenian– Bathonian interval from Óbánya compared with Southern Spain (from O'Dogherty et al. 2006), Cabo Mondego, Portugal (from

Suchéras-Marx et al. 2012); Chaudon Norante, SE France (from Suchéras-Marx et al., 2013); Wadi Naqab, United Arab Emirates (Hönig and John 2015) and the Umbria-Marche Basin, Italy(from Bartolini et al. 1999).

518
519
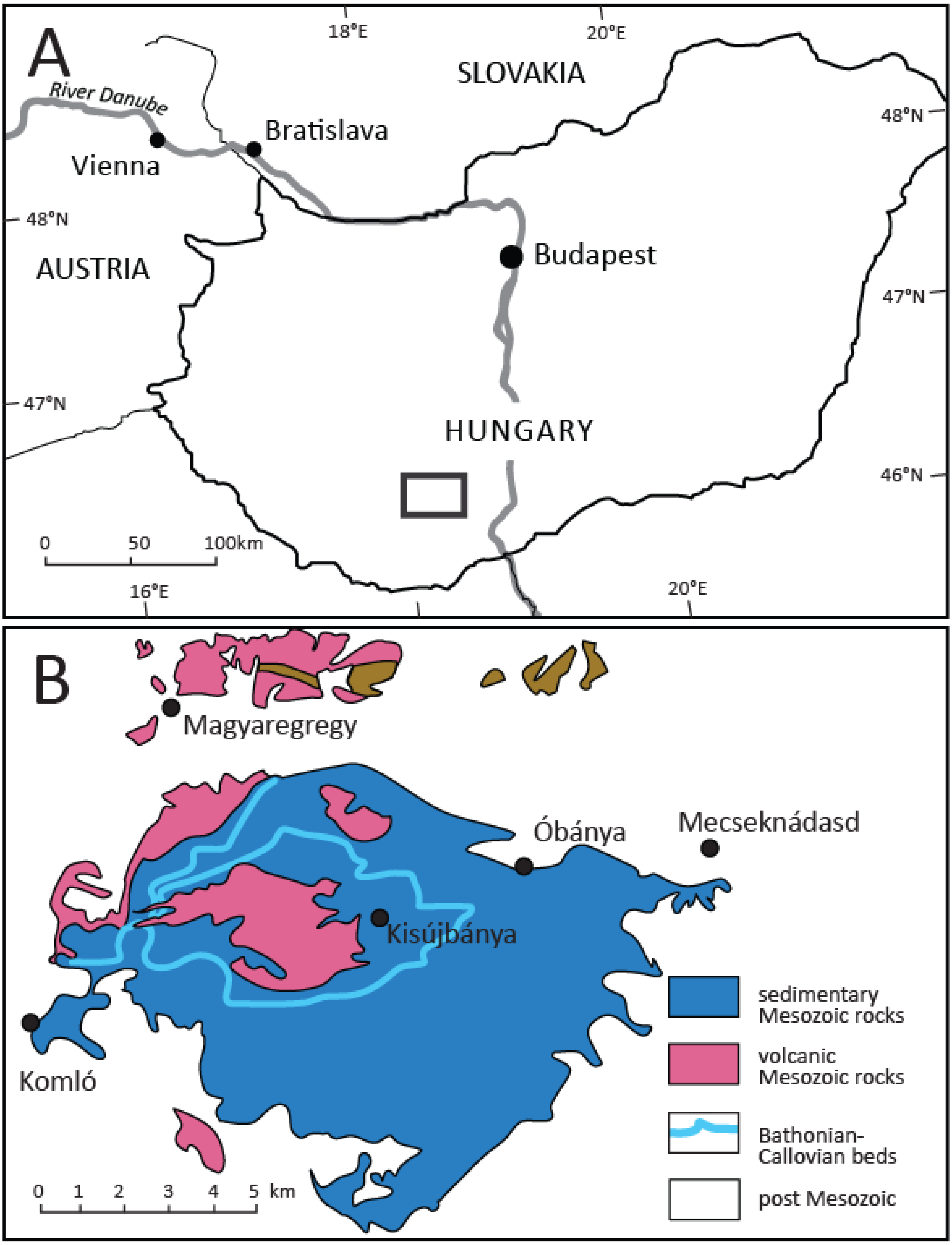

520 Figure 1

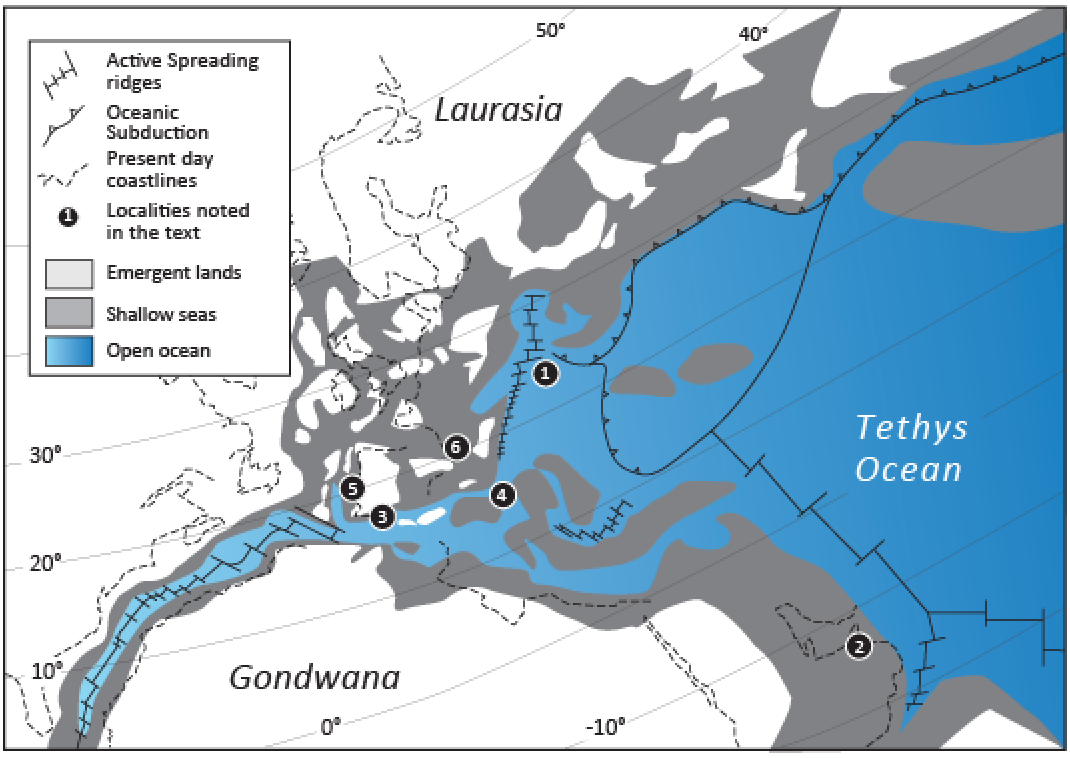
Active Spreading ridges
Oceanic Subduction
Present day coastlines
Localities noted in the text
Emergent lands
Shallow seas
Open ocean
Laurasia
Gondwana
Tethys Ocean
50°
40°
30°
20°
10°
0°
-10°
1
2
3
4
5
6

Figure 2

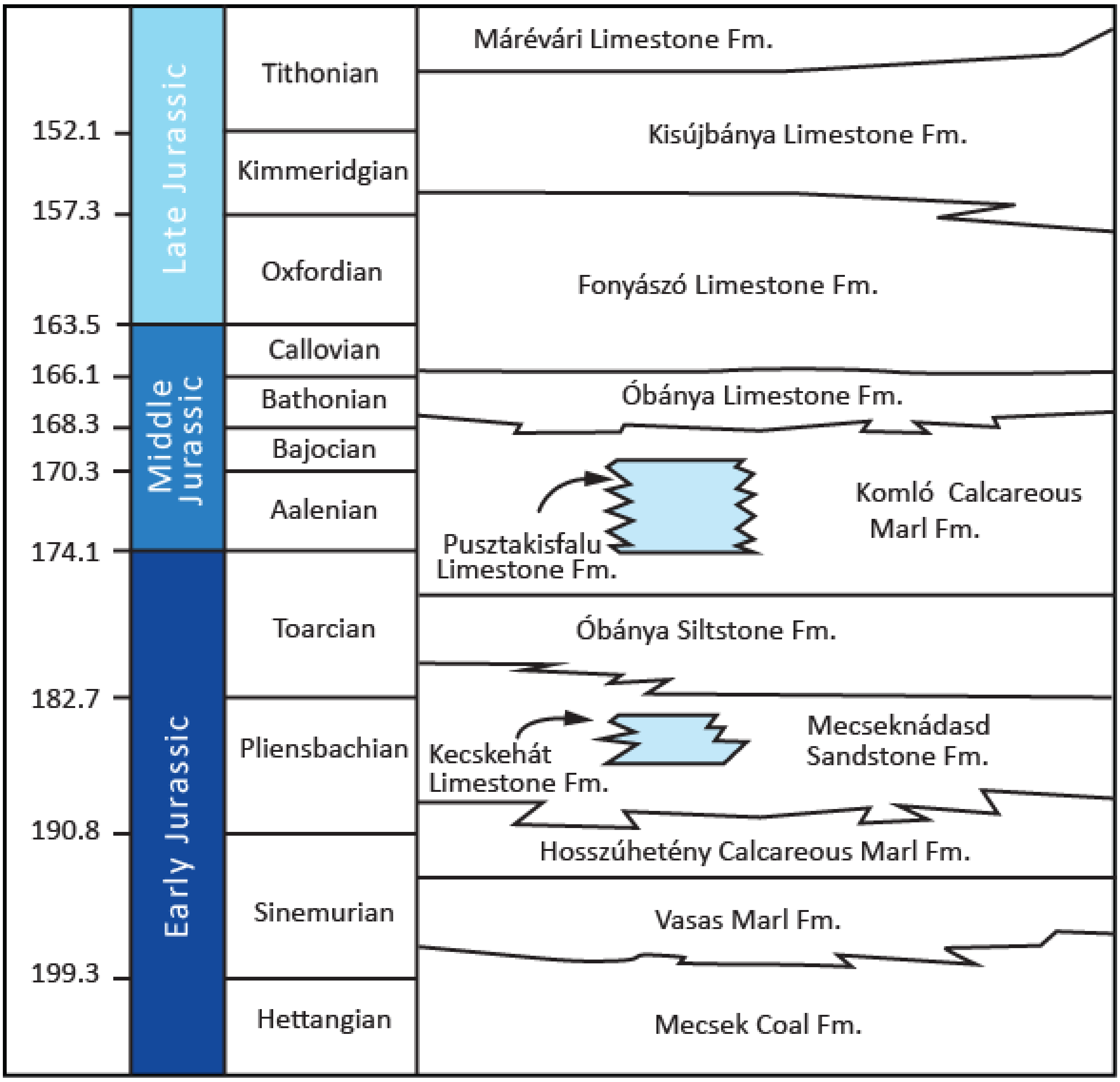

Late Jurassic
Middle Jurassic
Early Jurassic
152.1
157.3
163.5
166.1
168.3
170.3
174.1
182.7
190.8
199.3
Tithonian
Kimmeridgian
Oxfordian
Callovian
Bathonian
Bajocian
Aalenian
Toarcian
Pliensbachian
Sinemurian
Hettangian
Márévári Limestone Fm.
Kisújbánya Limestone Fm.
Fonyászó Limestone Fm.
Óbánya Limestone Fm.
Komló Calcareous Marl Fm.
Pusztakisfalu Limestone Fm.
Óbánya Siltstone Fm.
Mecseknádasd Sandstone Fm.
Kecskehát Limestone Fm.
Hosszúhetény Calcareous Marl Fm.
Vasas Marl Fm.
Mecsek Coal Fm.

Figure 3


A
B
C
D

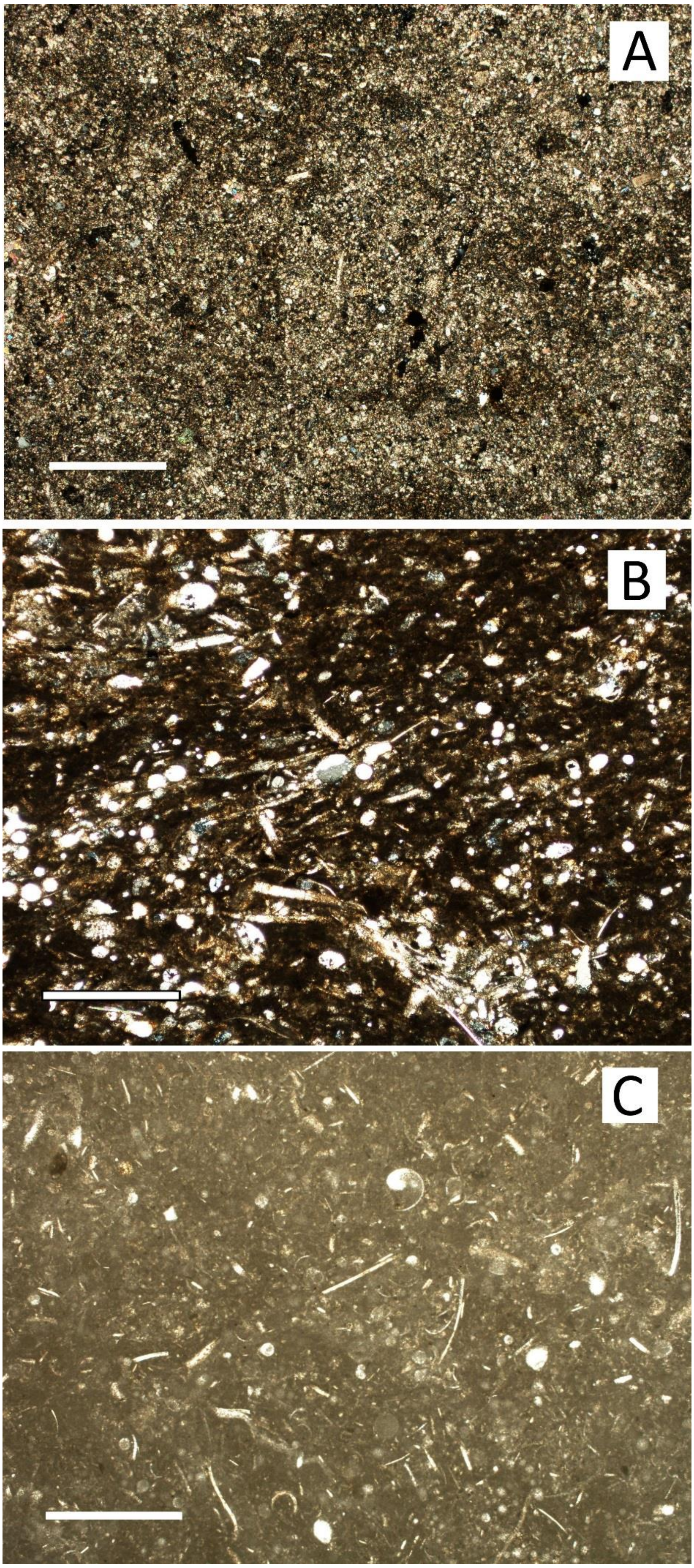
A
B
C

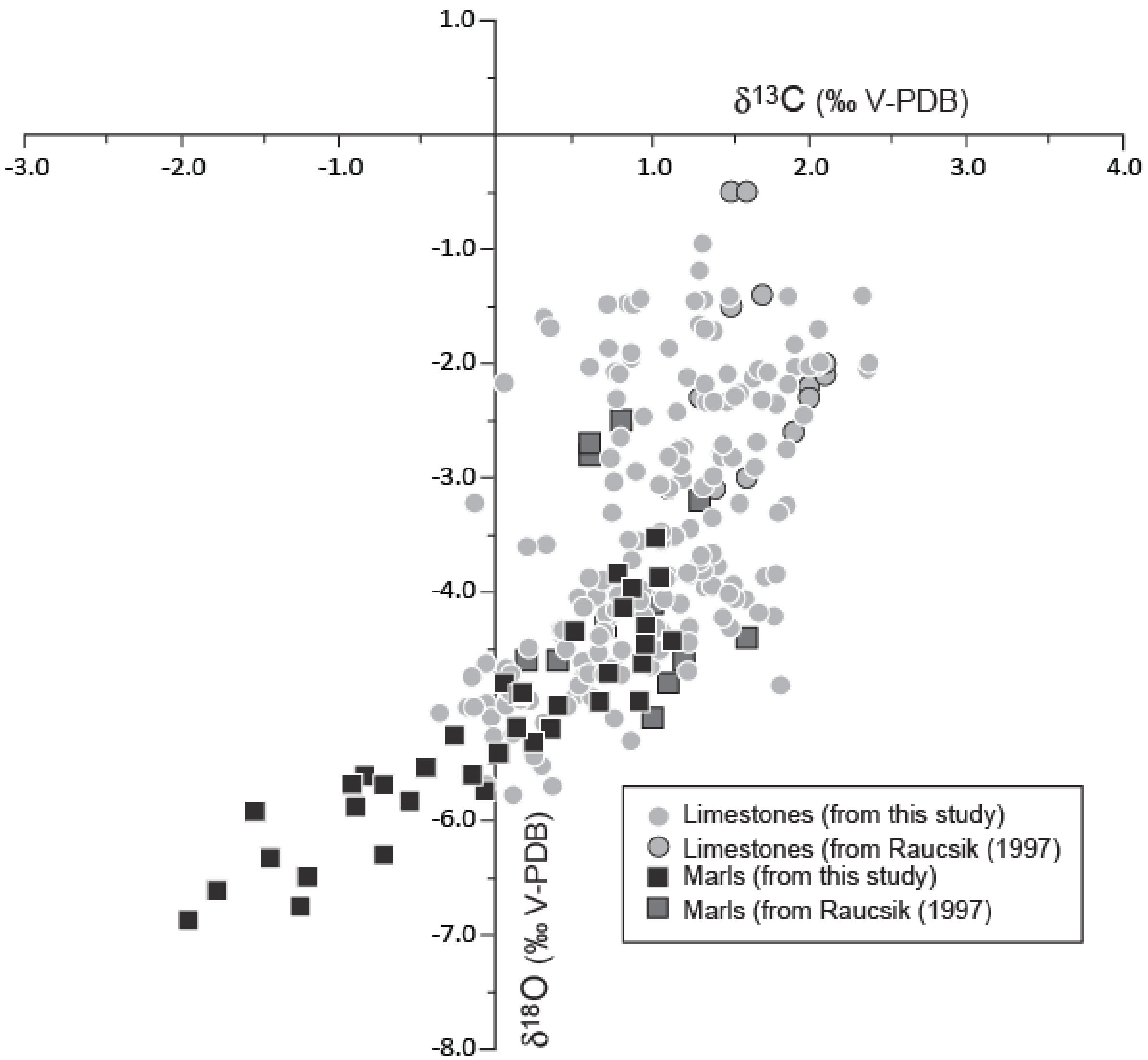
δ13C (‰ V-PDB)
δ18O (‰ V-PDB)
-3.0
-2.0
-1.0
1.0
2.0
3.0
4.0
1.0
-1.0
-2.0
-3.0
-4.0
-6.0
-7.0
-8.0
Limestones (from this study)
Limestones (from Raucsik (1997)
Marls (from this study)
Marls (from Raucsik (1997)

Figure 6

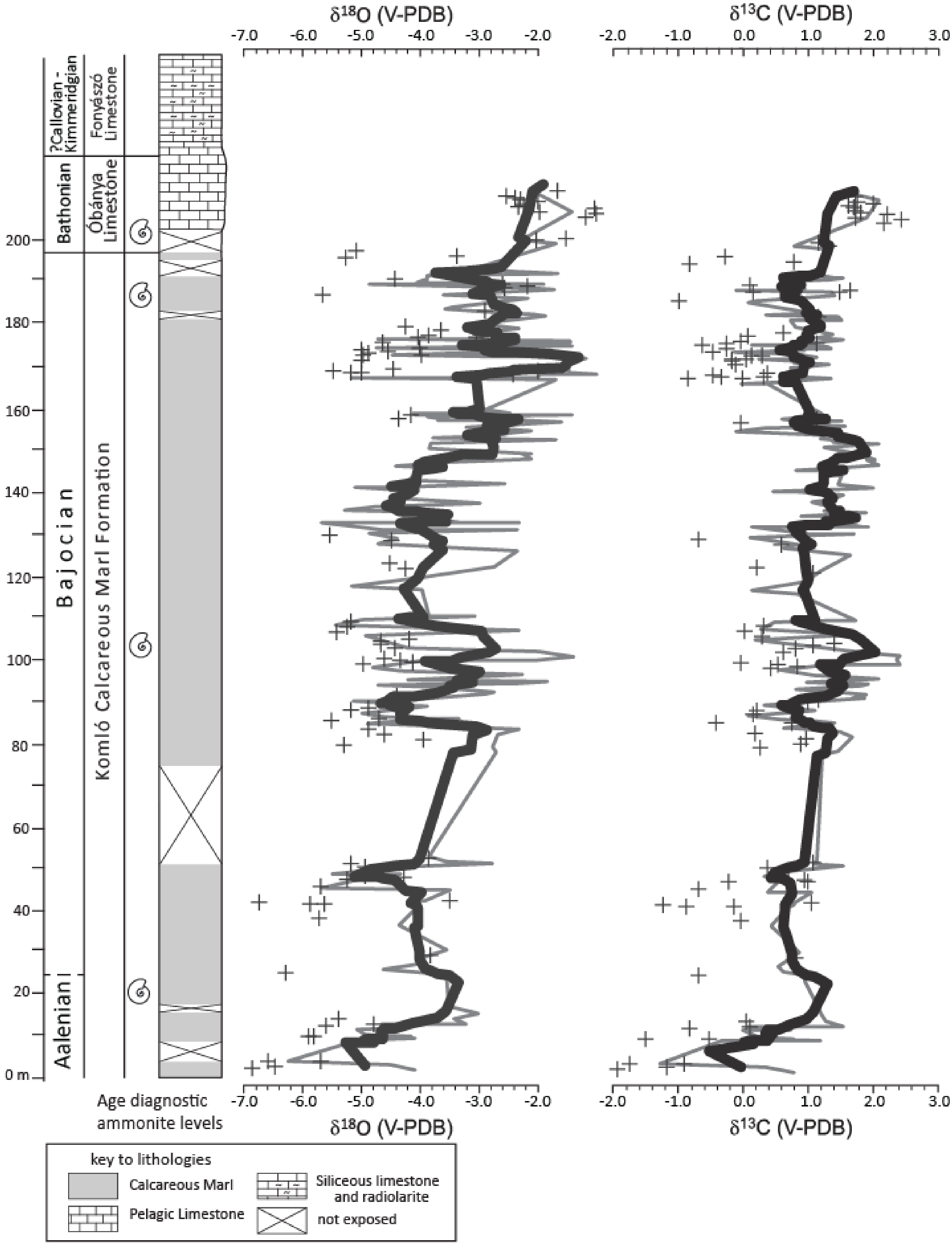

549
550 Figure 7
551

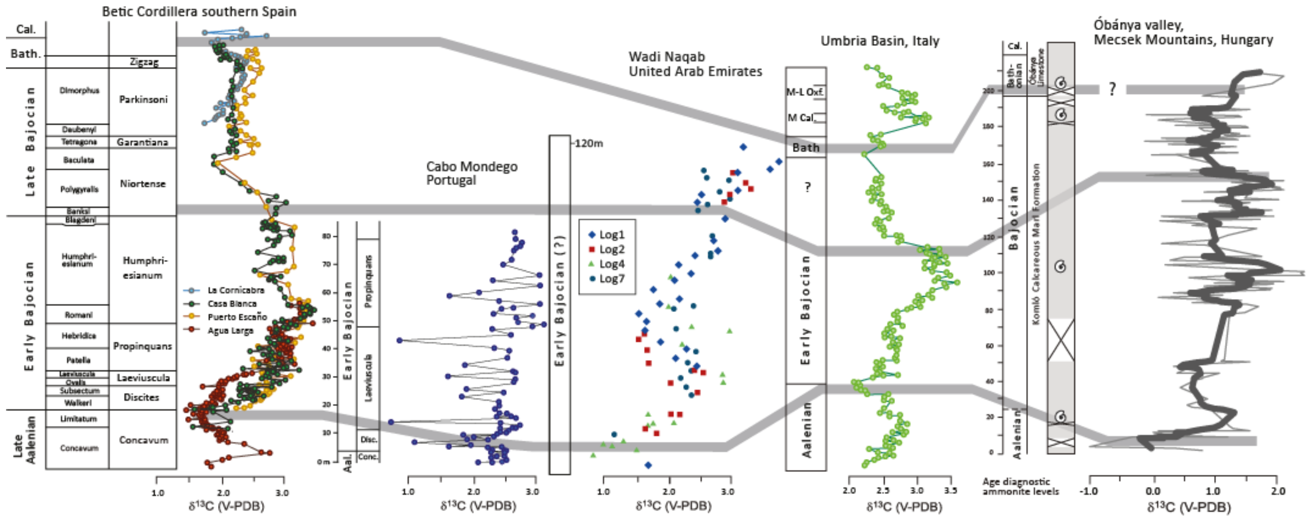
Betic Cordillera southern Spain
Cal.
Bath.
Late Bajocian
Early Bajocian
Late Aalenian
Zigzag
Parkinsoni
Garantiana
Niortense
Humphriesianum
Propinquans
Laeviuscula
Discites
Concavum
La Cornicabra
Casa Blanca
Puerto Escaño
Agua Larga
Cabo Mondego
Portugal
Early Bajocian (?)
120m
Wadi Naqab
United Arab Emirates
Log1
Log2
Log4
Log7
Umbria Basin, Italy
M-L Oxf.
M Cal.
Bath
?
Early Bajocian
Aalenian
Óbánya valley,
Mecsek Mountains, Hungary
Komló Calcareous Marl Formation
Age diagnostic ammonite levels
δ13C (V-PDB)

Figure 8